*Inorganica Chimica Acta*, 26 (1978) 213–220



# The Electronic Absorption Spectra of the Transition Elements Rh, Ir, Ni, Pd and Pt in Molten Cyanide

K. S. DE HAAS and K. F. FOUCHÉ
*National Nuclear Research Centre, Pelindaba, Private Bag X256, Pretoria, South Africa*
Received May 19, 1977

*Electronic absorption spectra were recorded on molten (Na, K)CN solutions containing rhodium, iridium, nickel, palladium and platinum, at temperatures exceeding 500 °C.*

*Only those complexes which have characteristic bands at energies lower than 340 nm could be identified; alkali cyanide absorbs strongly at higher energies. The low-oxidation state species, $Rh(CN)_4^{3-}$, and Rh(0)–cyanide, $Ir(CN)_4^{3-}$, and Ir(0)–cyanide complexes are present in the molten salt when the metals are dissolved as III- and I-oxidation state compounds. The complex Pd(I)–cyanide is formed when $PdCl_2$ is dissolved in the melt, while Pt(I)–cyanide and Pt(0)–cyanide are formed when $K_2PtCl_4$ is dissolved in the melt. An Ni(I) complex, $Ni_2(CN)_6^{4-}$, was identified in the molten cyanide to which $NiCl_2$ and Ni sponge had been added.*

*A description is also given of the spectroscopic equipment used, as well as of the graphite sample cell with diamond windows.*

## Introduction

Molten cyanide has recently been shown to be a useful solvent for platinum-group and related metals [1], and was also found to be effective in stabilising low-oxidation state metal cyanide complexes [2, 3]. Most of these complexes are strongly coloured, and electronic absorption spectra proved to be an efficient technique for studying the chemistry of metal-containing cyanide melts. So far [2, 3] only quenched cyanide melts have been investigated spectroscopically. This has now been extended to the study of molten samples containing Rh, Ir, Ni, Pd and Pt, which is described in this paper. A description is also given of the spectroscopic equipment and sample cell used in recording the electronic absorption spectra of molten cyanide solutions.

To the authors' knowledge, electronic absorption spectra have never before been recorded on molten cyanide solutions.

## Experimental

### *Apparatus*

#### *Spectrophotometer*

Most commercial spectrophotometers are not suitable for recording spectra at temperatures in excess of 500 °C, since polychromatic radiation, emitted by the sample cell and the furnace, heats the detector, resulting in excessive noise. In order to minimise this effect, a single-beam spectrophotometer with the following sequence of components was designed: LIGHT SOURCE–CHOPPER–LENS-1–FURNACE–LENS-2–INLET SLIT–MONOCHROMATOR–EXIT SLIT–DETECTOR–AMPLIFIER–PAPER RECORDER AND BCD PUNCH RECORDER.

The light source, chopper, lens-1 and furnace are all mounted onto a lathe bed, which in turn is bolted onto a flat aluminium tray. Lens-2 and the monochromator are firmly fixed to a sturdy iron table. The detector and the inlet and exit slits (the two slits are coupled) are attached to the monochromator. The flat aluminium tray is mounted on rails attached to the iron table. In moving the aluminium tray backward and forward across the light path of the spectrophotometer, the light source can be aligned with the detector. The light source can furthermore be adjusted horizontally and vertically with respect to the position on the lathe bed.

The furnace is centred on the focus point of lens-1, and the other components photometrically aligned.

The light source consists of a 6 V, 30 W tungsten lamp. The direct-drive chopper rotates at 50–60 Hz at 115 V. Lens-1 and lens-2 are both 3.2 cm diameter quartz lenses, the first spherical and the latter cylindrical. A Jarrell–Ash monochromator Model 82-000 Serial No. EU-D-1, with a diffraction grating of 1180 grooves/mm and blazing angle of 3000 Å is used. The inlet and exit slits are manually adjusted by turning a screw which is calibrated in microns by turning a vernier screw. The detector consists of an R456-type photomultiplier tube. The signal from the PM

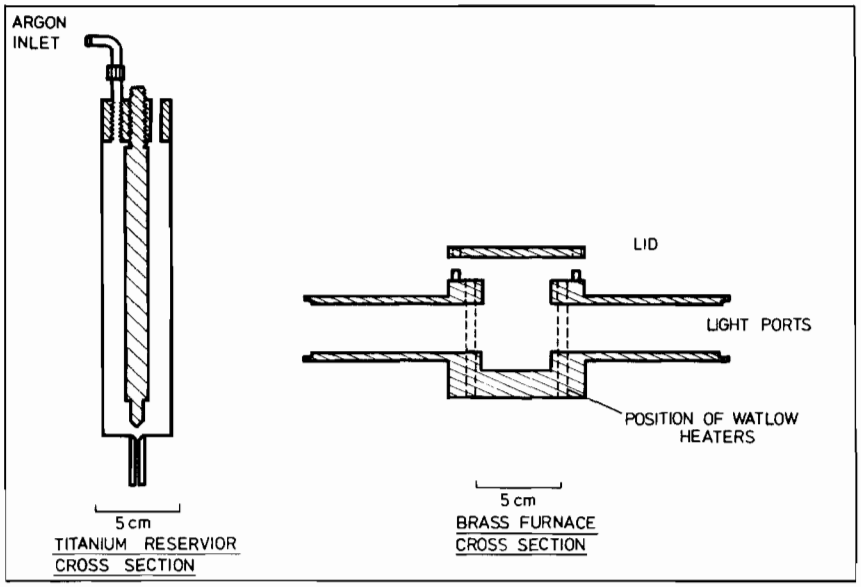


Figure 1. Exploded views of the titanium furnace and reservoir.

tube is amplified to a maximum output of 23 mV. A dark-current control is available to cancel out the residual current of the PM tube. The output signal is recorded on a Beckman multirange paper-recorder, and simultaneously stored on paper tape as BCD output.

*Furnace*

The brass furnace assembly is shown schematically in Fig. 1. It is composed of two cylindrically shaped light-beam ports of ID 3 cm and length 8.5 cm, attached to opposite sides of a central brass block with external dimensions 8 cm × 8 cm × 7 cm. The graphite sample cell (see below) is housed in a cylindrical hole of diameter 4 cm centred in the central block and milled to a depth of 5.4 cm. A brass lid which can be removed by loosening four nuts permits easy access to the sample-cell housing. A silver washer positioned between the lid and brass block helps to seal off the sample-cell housing. The brass block is heated by six Watlow heaters (type G 3 Ax346 A with diameter 9.4 mm and maximum wattage input of 120 V 250 W) which are spaced in a circle concentric with the sample-cell housing. The Watlow heaters are activated by two Variacs. The temperature of the furnace in the vicinity of the sample-cell housing is measured with an iron-constantan thermocouple. The light-beam ports are closed off by two spectroscopic-quality quartz windows, supported between flat graphite washers and tightened to the casing of the light-beam ports by two metal ring nuts. An argon flow (oxygen content $< 10$ ppm) is maintained through the furnace, entering the light-beam ports near the windows and leaving through a hole in the brass lid; the "pipette" of the reservoir passes through this hole (see below). The furnace is encased in vermiculite and firebrick insulation.

*Reservoir*

Gas bubbles frequently formed between the two diamond windows (see below) when the pulverised alkali-cyanide eutectic was melted directly in the graphite sample cell. The presence of such bubbles in the light path drastically affected the profile of the energy-response curve. This problem was overcome by first melting the anhydrous cyanide eutectic in a reservoir, which is schematically shown in Fig. 1, and running the molten cyanide dropwise into the graphite cell.

The titanium reservoir consists of a pipe (4.1 cm ID. and 20 cm long) attached to a "pipette" (5 mm OD. and 3 cm long) through which a hole 1 mm in diameter is drilled. A titanium plug which screws into the other end of the pipe supports a titanium rod (see Fig. 1). The "pipette" is sealed off when the titanium rod is screwed clockwise through the titanium plug until the cone-shaped point of the rod fits tightly into a seat, of similar shape, machined out of the base of the pipe. The reservoir is filled through a hole in the titanium plug.

The reservoir is heated in a Nikrothal wire-wound furnace which is mounted onto the brass furnace in such a way that the "pipette" of the reservoir passes through a hole in the lid of the brass furnace. A positive pressure of argon (oxygen content $< 10$ ppm) is maintained in the reservoir when it is in this position.

*Graphite Cell*

The sample cells, schematically shown in Fig. 2, were manufactured out of reactor-grade graphite and are cylindrically shaped (3.8 cm OD. and 5.3 cm long). The melt is contained within a cylindrical hole (forthwith known as the "sample hole") 6.0 mm in diameter and 3.1 cm in length, opening up to a

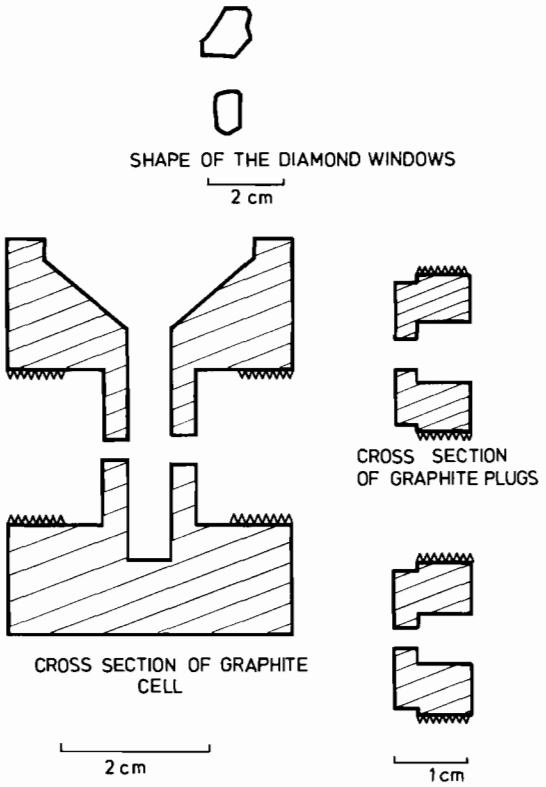


Figure 2. Exploded view of the graphite cell.

truncate-shaped reservoir at the top of the cell. The light beam passes through two holes of diameter 2.8 mm and 3.8 mm respectively (the diameter of each hole is determined by the size of the diamond which must cover it) drilled through the walls of the "sample hole". These holes are closed off by two diamond windows (Type IIA with thickness 1 mm) which fit into depressions milled out to a depth of 0.7 mm and according to the shape of the diamonds on the external wall of the "sample hole". The diamond windows are tightened to the wall of the depressions by graphite plugs which screw into holes milled out of the sample cell.

The sample cells were capable of containing molten cyanide for at least 3 h.

*Experimental Procedures*

The effect of total rhodium concentration on the ratio of $Rh(CN)_6^{3-}$ to $Rh(CN)_4^{3-}$ in molten cyanide was studied by measuring the relative heights of the IR peaks at 2145 $cm^{-1}$ ($Rh(CN)_6^{3-}$) and at 2055 $cm^{-1}$ ($Rh(CN)_4^{3-}$). The quenched melts were prepared by melting silicon-purified (Na, K)CN [4] and $RhCl_3$ together in a high-purity glove box [2] for 3 h and then quenching the metal-containing melt. The infrared spectra were recorded on a Perkin–Elmer 467 grating spectrophotometer. The procedures which were followed in preparing the samples have been described previously [2].

*Preparation of Samples*

The preparation of the compounds $RhCl_3$, $IrCl_3$ and $Ir(PPh_3)_2$ COCl is described in ref. 2. The other metal salts were commercially available.

The reservoir was filled in a high-purity glove box [2]. The (Na, K)CN eutectic was vacuum-dried (1,3 Pa) for three days and then transferred to the glove box. Samples of metal salts in (Na, K)CN were prepared by pulverising the mixture in an agar mortar. The nickel-containing melts were diluted from quenched melts prepared by first melting anhydrous $NiCl_2$ and nickel sponge in the molar ratio of 1, together with (Na, K)CN), and then filtering the melt through a sintered-glass frit.

*Procedure Followed in Recording Spectra*

The graphite cell, dried overnight at 120 °C, is positioned in the brass furnace. After the brass lid has been fastened to the central block, the Nikrothal wire-wound furnace is positioned on top of the brass furnace. The temperature of each furnace is increased, and a flow of argon passed through the brass furnace. After both furnaces have reached a temperature of 540 °C, the reservoir is taken out of the glove box and positioned in the wire-wound furnace.

With the sample cell, reservoir and wire-wound furnace in this position, the spectrophotometer is photometrically aligned. The energy-response curve of the empty cell is then recorded on tape and on the Beckman paper-recorder over the wavelength range, 650–340 nm. In an attempt to flatten the profile of the energy-response curve, the inlet and exit slits are manually adjusted at certain fixed wavelengths.

After the temperature of the reservoir has been held at 540 °C for 30 min, the melt is added dropwise to the graphite sample cell (a period of 30 min was found to be sufficient for the melt to attain homogeneity). The energy-response curve of the melt-containing cell is recorded with the slits adjusted at the same wavelength settings as before, except that larger slits are now required. In all cases the recording of the energy-response curve of a melt was preceded by the recording of the energy-response curve of the empty sample cell. Furthermore, the spectrophotometer was held in the same "aligned" position in recording these two energy-response curves. The relative-absorbance curve of the melt is calculated by dividing the energy-response curve of the empty cell by the energy-response curve of the melt-containing cell.

The solute-absorbance curve is calculated by subtracting the relative-absorbance curve of the pure-cyanide melt from the relative-absorbance of the

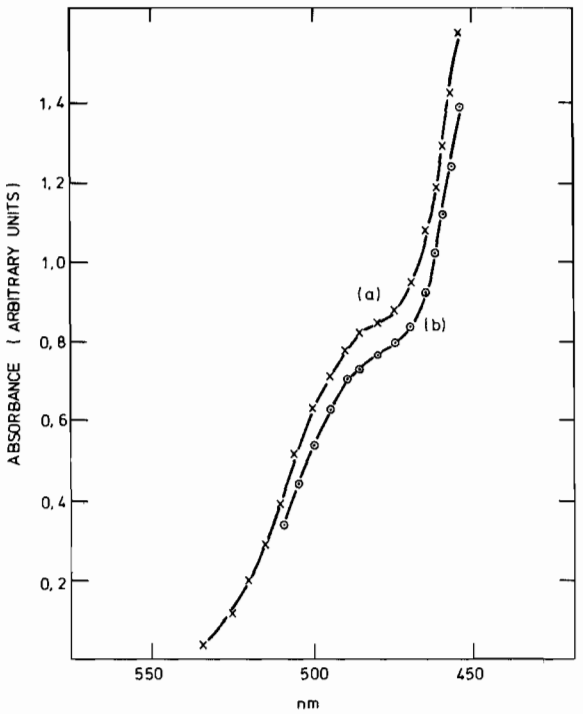


Figure 3. Electronic absorption spectra of a molten cyanide solution containing iridium ([Ir] = 2.18 × $10^{-3}$ *M*). (a) at 573 °C; (b) at 545 °C.

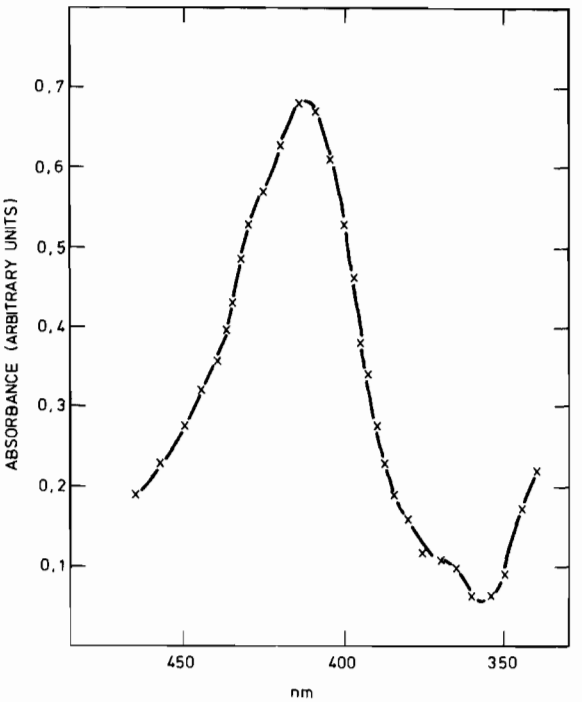


Figure 4. Electronic absorption spectrum of a molten cyanide solution containing iridium ([Ir] = 6.6 × $10^{-5}$ *M*) at 555 °C.

metal-containing melt. The same slit openings are used to record the energy-response curves of the pure-cyanide and the metal-containing melts. Furthermore, the slits were adjusted at the same fixed wavelength settings in recording the energy-response curves of the empty cell, pure-cyanide and metal-containing melts.

Following this procedure, the electronic spectra of aqueous solutions containing $NiSO_4 \cdot 7H_2O$ and $K_2PtCl_4$, were recorded at room temperature. The position and extinction coefficients of the bands observed for $NiSO_4 \cdot 7H_2O$ (400 nm ($\epsilon$ = 5.2) and 660 nm ($\epsilon$ = 2.2)) and $K_2PtCl_4$ (475 nm($\epsilon$ = 15), 393 nm ($\epsilon$ = 56) and 330 nm ($\epsilon$ = 61)) agree favourably with the reported spectra of $NiSO_4 \cdot 7H_2O$ [5] (397 nm ($\epsilon$ = 5.0) and 660 nm ($\epsilon$ = 2.0)) and $K_2PtCl_4$ [6] (475 ($\epsilon$ = 16), 392 ($\epsilon$ = 58) and 328 nm ($\epsilon$ = 64)).

## Results and Discussion

The spectra recorded on the metal-containing melts were interpreted with the aid of the diffuse-reflectance spectra recorded on similar melts which had been quenched [2, 3].

The density of the eutectic-cyanide melt [7] as a function of temperature has been formulated as $\rho$ = 1.497 − 4.145 × $10^{-4}$ × t.

Although the cyanide melt is practically transparent in the visible region, its absorbance curve increases sharply at energies exceeding 340 nm.

Whereas sodium cyanamide (increasing the reduction potential of molten cyanide) or sodium dicyanamide (decreasing the reduction potential of molten cyanide) was previously [2, 3] added to the metal-containing melts in order to minimise the number of species present, molten-cyanide solutions containing these compounds at a concentration higher than 1% (by weight with respect to cyanide) absorb strongly at energies greater than 25000 $cm^{-1}$.

*Iridium*

The electronic absorption specra of iridium-containing melts are shown in Fig. 3 ([Ir] = 2.18 × $10^{-3}$ *M*, dissolved as $IrCl_3$ or $Ir(PPh_3)_2COCl$) and Fig. 4 ([Ir] = 6.6 × $10^{-5}$ *M*, dissolved as $IrCl_3$). The sepctra are characterised by a prominent shoulder at 485 nm, and a complex band which can be resolved into the bands at 430 nm (shoulder), 413 and 370 nm (shoulder).

The spectra shown in Figs. 3 and 4 are very similar to that part of the diffuse-reflectance spectrum (Fig. 6 in ref. 2) (bands at 560, 470, 425 nm (shoulder), 400 and 365 nm (shoulder)) at energies lower than 340 nm, recorded on iridium-containing quenched melts, except for a bathochromic shift of all the absorption bands and the absence of a band in the vicinity of 560 nm. A bathochromic shift of absorption bands with increase in temperature is to be expected. It was experimentally observed that the intensity of the purple colour

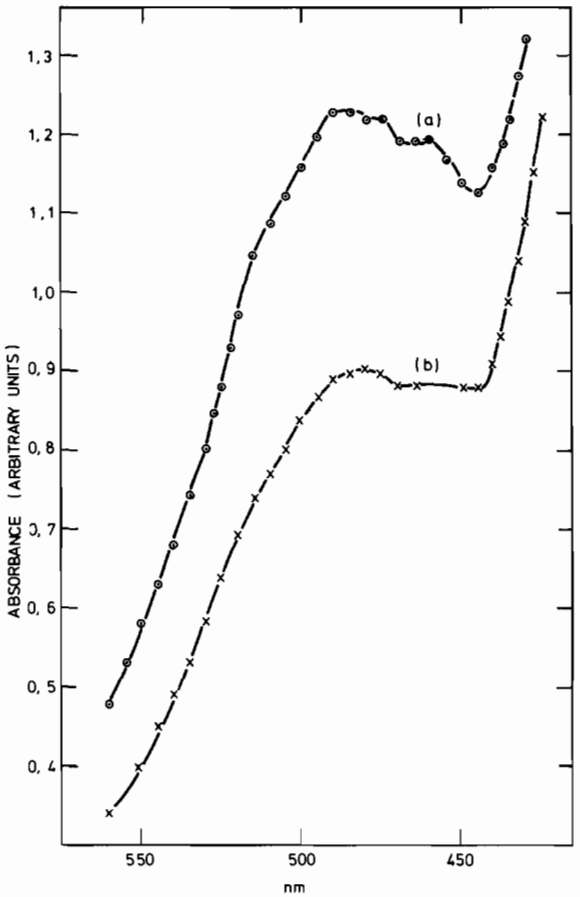


Figure 5. Electronic absorption spectra of a molten cyanide solution containing nickel ([Ni] = $3.9 \times 10^{-4}$ *M*). (a) at 567 °C; (b) at 516 °C.

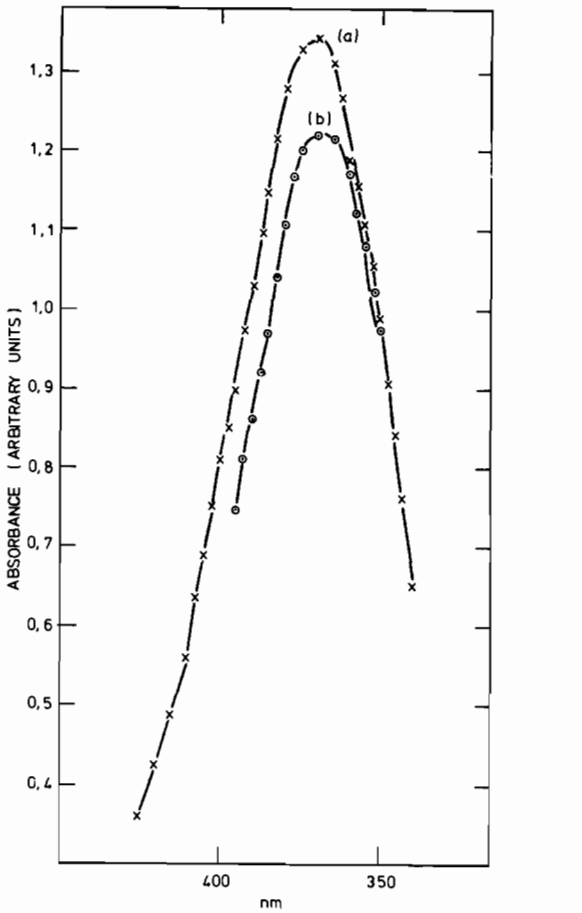


Figure 6. Electronic absorption spectra of a molten cyanide solution containing nickel ([Ni] = $6.5 \times 10^{-5}$ *M*). (a) at 565 °C; (b) at 517 °C.

(associated with the 560 nm band) of a quenched cyanide-melt containing a high concentration of an Ir(0)–cyanide complex (for more details of these quenched melts see ref. 2), decreased with increase in temperature until, in the molten state, the melt assumes a yellowish colour.

The spectra shown in Figs. 3 and 4 can therefore be interpreted on the basis of the diffuse-reflectance spectrum shown in Fig. 6 of ref. (2), as a composite of the spectra of the two species $Ir(CN)_4^{3-}$ (bands at 485, 430, and 370 nm) and a Ir(0)–cyanide complex (band at 413 nm).

The increase in intensity of the band at 485 nm with increase in temperature (Figs. 3(a)–(b)) indicates that the transition is probably vibronically coupled.

*Nickel*

Previously [3] it was shown that $Ni(CN)_4^{2-}$ and $Ni(CN)_4^{4-}$ are formed if Ni(II) salts are melted together with eutectic cyanide. However, neither of these species absorb at energies less than 340 nm. On the other hand $Ni_2(CN)_6^{4-}$, which is formed when Ni(II) salts and nickel sponge are melted together with eutectic cyanide, absorbs strongly at energies less than 340 nm [3]. Only the spectra of the melts prepared according to the last method could therefore be recorded.

The spectra recorded on nickel-containing melts prepared by adding nickel sponge and Ni(II) compounds to the melt are given in Figs. 5 ([Ni] = $3.9 \times 10^{-4}$ *M*) and 6([Ni] = $6.5 \times 10^{-5}$ *M*). The spectra are characterised by an intense band at 370 nm and a complex band with maximum at 495 nm which can be resolved into bands at 515, 495 and 460 nm. These spectra are similar to that portion of the diffuse-reflectance spectra at energies greater than 325 nm (*i.e.* the bands at 340 and 470 nm) recorded on the isolated $Ni_2(CN)_6^{4-}$ complex [3] and on the quenched melt prepared by melting Ni(II) compounds and nickel sponge together with (Na, K)-CN (Fig. 1(b) in ref. 3). The bathochromic shift of the bands (470 to 495 nm and 340 to 370 nm) is to be expected for the large difference in temperature between the two media. The resolution of the broad 470 nm band in the quenched-melt spectrum into three bands in the molten-salt spectrum can be

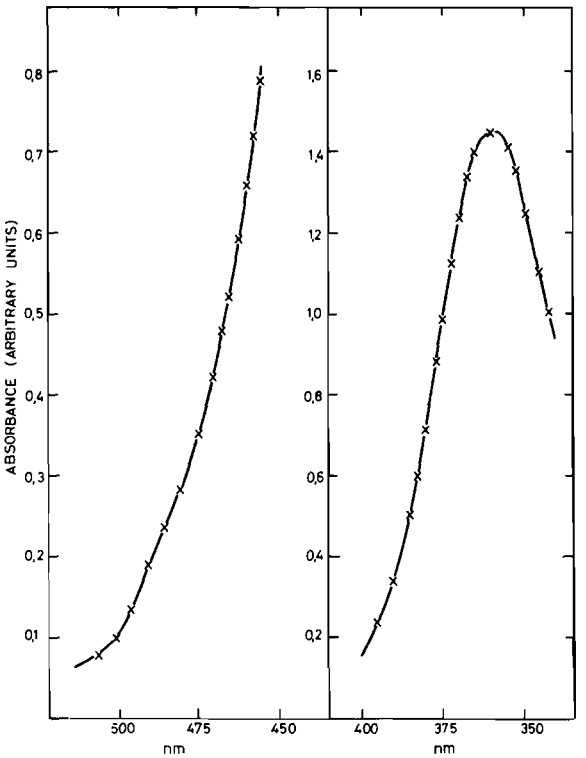


Figure 7. Electronic absorption spectra of a molten cyanide solution containing palladium at 540 °C. (a) [Pd] = 1.55 × $10^{-2}$ *M*: (b) [Pd] = 7.3 × $10^{-4}$ *M*.

accounted for if the transitions which are associated with the bands at 515, 495 and 460 nm, have different temperature-dependencies; the change in the energy profile of the spectrum recorded at 516 °C (Fig. 5(b)) compared with that recorded at 567 °C (Fig. 5(a)) supports this. The above results show that the complex $Ni_2(CN)_6^{4-}$ is present in the melt.

The increase in the intensity of all the bands shown in Figs. 5 and 6 with increase in temperature can be explained only if these bands are categorised as vibronically allowed transitions.

*Palladium*

The complexes $Pd(CN)_4^{2-}$ and $Pd(CN)_4^{4-}$ which could be present in quenched melts [3] absorb at energies much greater than 340 nm. On the other hand it should be possible to observe whether the Pd(I)–cyanide complex is present in the melt, because its diffuse-reflectance spectrum (Fig. 3(a) in ref. 3) is characterised by bands at 580 nm (weak), 444 and 340 nm.

The electronic absorption spectra recorded on palladium-containing melts when palladium is dissolved as anhydrous $PdCl_2$, are shown in Figs. 7(a) ([Pd] = 1.55 × $10^{-2}$ *M*) and 7(b) ([Pd] = 7.3 × $10^{-4}$ *M*). The spectra are characterised by an intense peak at 360 nm which partly conceals an absorption hand with much lower intensity, appearing as a shoulder at 485 nm.

The positions of these bands (485 and 360 nm) are in good agreement with those of the two bands at 444 and 340 nm which were recorded on the quenched cyanide-melt (Fig. 3(a) in ref. 3), except for a bathochromic shift of the latter bands. It was observed in practice that the intensity of the orange–yellow colour (associated with the 444 nm band) of the quenched melt decreased with increase in temperature; this explains why the 444 nm band, which is prominent in the diffuse-reflectance spectra [3], appears as a shoulder at 540 °C. It can therefore be concluded that the same Pd(I)–cyanide complex which was identified in the quenched cyanide melt [3], is also present in the melt.

*Platinum*

The spectra recorded on platinum-containing melts when platinum is dissolved as $K_2PtCl_4$, are shown in Figs. 8 ([Pt] = 3.6 × $10^{-3}$ *M*) and 9 ([Pt] = 7 × $10^{-4}$ *M*). Contrary to the observations on Ir, Ni and Pd, the spectra of platinum-containing melts changes with time at constant temperature, as is shown in Fig. 9 (a, b). The spectrum (peak at 355 nm and a shoulder at 370 nm) changes to a different spectrum (peak at 370 nm and shoulder at 355 nm); this is accompanied by an increase in the intensity of the shoulder at ~418 nm. The rate of these spectral changes is enhanced when the flow rate of argon through the furnace is decreased.

The observed spectral changes with time are probably due to the oxidation of low-oxidation state platinum complexes to higher-oxidation states. This explanation seems plausible, since the inert atmosphere in the titanium reservoir is certainly better than the prevailing atmosphere in the graphite cell during the time of recording. It is further supported by the observation that the change can be enhanced by lowering the argon flow through the cell. The main source of contamination is probably through the graphite seals on the quartz windows, which could not be made vacuum-tight.

Since $Pt(CN)_4^{2-}$ absorbs at energies higher than 340 nm [3], it cannot be associated with the spectra shown in Figs. 8 and 9. On the other hand, it is known [3] that the Pt(I)–cyanide complex (Fig. 7(b) in ref. 3) is characterised by bands at ~410, ~380 and 340 nm; the first two bands are part of a poorly resolved complex band, with maximum at ~400 nm. Furthermore, a Pt(0)–cyanide complex (bands at 280 and 350 nm), which decomposed, upon exposure to the atmosphere, to the Pt(I)–cyanide complex, was also identified in the quenched melt [3]. The spectral changes shown in Figs. 9 (a, b) can therefore also be explained as the oxidation of a Pt(0)–cyanide complex (band at 355 nm) to a Pt(I)–cyanide complex (bands at 370 and ~418 nm).

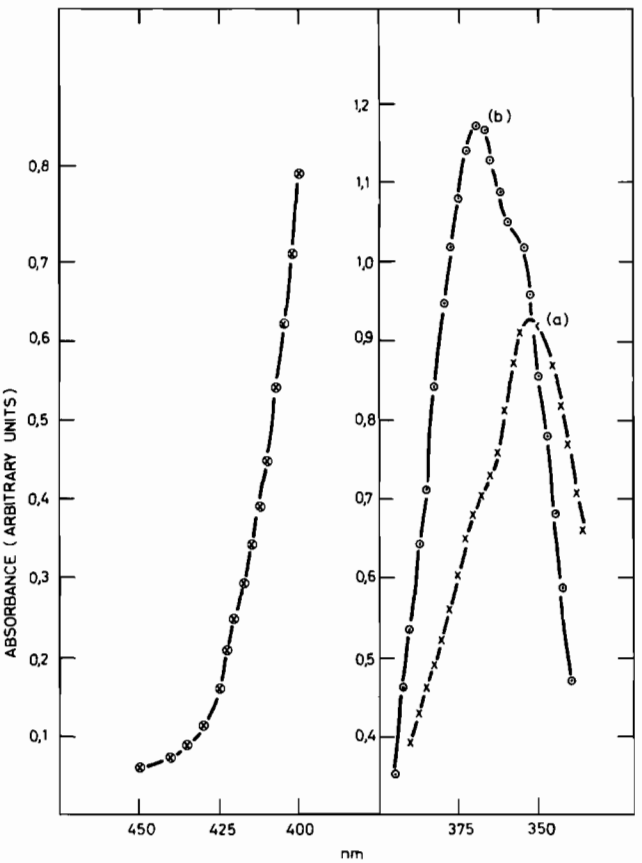


Figure 8. Electronic absorption spectrum of a molten cyanide solution containing platinum ([Pt] = $3.6 \times 10^{-3}$ *M*) at 540 °C.

Figure 9. Electronic absorption spectra of a molten cyanide solution containing platinum ([Pt] = $7 \times 10^{-4}$ *M*) at 540 °C. (a) Immediately after running in the melt; (b) 60 min later.

As in the case of palladium, the intensity of the yellow colour (associated with the ~410 nm band) of the quenched melt decreased with increase in temperature, which explains why the bands at ~410 and ~380 nm appeared as a peak in the diffuse-reflectance spectrum, but as a shoulder (~418 nm) in the molten cyanide.

*Rhodium*

The spectra recorded on a rhodium-containing melt ([Rh] = $2 \times 10^{-4}$ *M*) when rhodium is dissolved as $RhCl_3$ is shown in Fig. 10. The spectrum is characterised by a complex band which can be resolved into the three bands at 398 (shoulder), 370 and 345 nm (shoulder).

This spectrum differs appreciably from the diffuse-reflectance spectrum (Fig. 1(a) in ref. 2) recorded on rhodium-containing quenched melts; the bands at 390 nm and 310 nm were assigned to a $Rh(CN)_4^{3-}$ species, the bands at 444 and 360 nm to a Rh(0)–cyanide complex and the band at 220 nm to the $Rh(CN)_6^{3-}$ species. However, the diffuse-reflectance spectra were recorded on quenched melts containing rhodium in the concentration range 100–20 (molar ratio (Na, K)-CN to Rh), which is far more concentrated than the melts (molar-ratio range ~100 000) on which the spectra at 540 °C were recorded. The ratio of unreduced to reduced rhodium species decreases

TABLE I. The Ratio of the Height of the 2145 $cm^{-1}$ IR Band ($Rh(CN)_6^{3-}$) to the Height of 2055 $cm^{-1}$ IR Band ($Rh(CN)_4^{3-}$) as a Function of Rhodium Content (expressed as molar ratio, (Na, K)CN to $RhCl_3$).

| $I_{2145}/I_{2055}$ | Molar Ratio, (Na, K)CN:$RhCl_3$ |
|---|---|
| 0.26 | 300 |
| 0.92 | 150 |
| 1.62 | 98 |
| 1.74 | 78 |
| 2.02 | 50 |
| 2.32 | 28 |
| 4.00 | 9.5 |

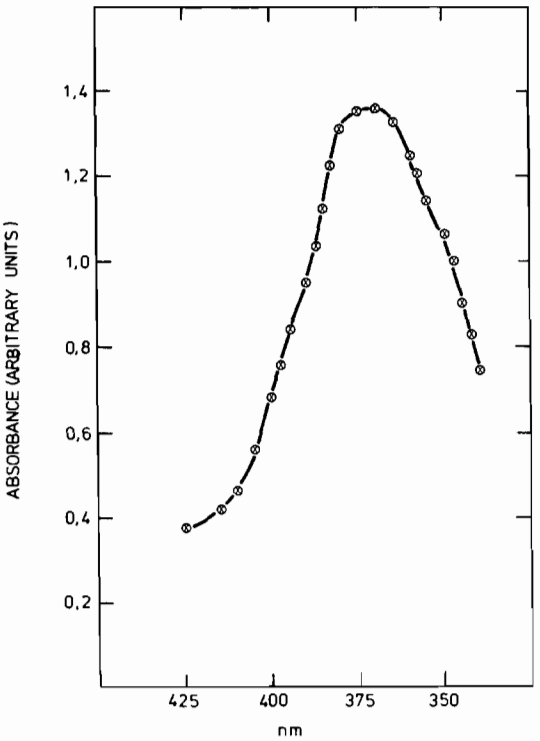


Figure 10. Electronic absorption spectra of a molten cyanide solution containing rhodium ([Rh] = $2 \times 10^{-4}$ *M*) at 540 °C.

substantially with an increase in dilution of rhodium content. This effect is clearly indicated in Table I by the change in the ratio of the height of the infrared bands at 2145 $cm^{-1}$ (characteristic of $Rh(CN)_6^{3-}$) and 2055 $cm^{-1}$ (characteristic of $Rh(CN)_4^{3-}$) as a function of molar ratio of (Na, K)CN to $RhCl_3$ (a plot of the ratio of the peak heights against rhodium concentration follows a hyperbola). This effect is to be expected, since the amount of dicyanamide which forms in the melt from the reduction of Rh(III), according to eq. 1 (see also ref. 2),

$$Rh(III) + 3CN^- \longrightarrow Rh(I) + C_2N_3^- + C, \qquad (1)$$

and from a further reduction of Rh(I) as follows:

$$2Rh(I) + 3CN^- \longrightarrow 2Rh(0) + C_2N_3^- + C \qquad (2)$$

should decrease with a decrease in the amount of $RhCl_3$ initially added to the melt. It is known [2] that dicyanamide decreases the reduction potential of the cyanide melt. It should therefore be expected that the concentration of Rh(III) species present in the melt would decrease with an increase in dilution.

From the data given in Table I it is likely that no $Rh(CN)_6^{3-}$ is present in the cyanide melt containing $2 \times 10^{-4}$ molar rhodium. The absence of $Rh(CN)_6^{3-}$ in such a melt is substantiated by the similarity to the spectrum shown in Fig. 10, both in profile and intensity, of a spectrum recorded on a melt prepared by electrolysing rhodium into the melt. It was shown [2] that the rhodium dissolved anodically as Rh(I). The spectrum shown in Fig. 10 must therefore be a composite of the spectra of a Rh(I) and an Rh(0) species (the possibility that the spectrum shown in Fig. 10 is caused by the absorption of dicyanamide formed as a result of the reduction of the Rh(III) species can be excluded, since a molten cyanide solution to which 0.05% sodium dicyanamide (by weight with respect to cyanide) had been added did not absorb more in this region than a pure cyanide melt. The concentration of 0.05% is substantially more than the amount of dicyanamide which could form according to eq. 1 from $2 \times 10^{-4}$ *M* Rh(III)).

In the same manner it can also be argued that the ratio of the two reduced species (Rh(I) to Rh(0) in the melt should decrease with an increase in dilution of rhodium in the melt. In agreement with this argument, the 370 nm band can possibly be assigned to the Rh(0)–cyanide complex, and the shoulders at 345 and 398 nm ascribed to the presence of some $Rh(CN)_4^{3-}$ in the melt.

## Acknowledgement

The authors are indebted to the Anglo American Corporation for the loan of the two diamonds, and the Atomic Energy Board for permission to publish these results.

## References

1 K. F. Fouché, J. G. V. Lessing and P. A. Brink, *"Proceedings of International Solvent Extraction Conference, Lyon, September 1974"*, Society for Chemical Industry, London (1974) pp. 2685.
2 K. S. de Haas, C. M. Fouché and K. F. Fouché, *Inorg. Chim. Acta, 21,* 15 (1977).
3 K. S. de Haas and K. F. Fouché, *Inorg. Chim. Acta, 24,* 269 (1977).
4 J. G. V. Lessing, K. F. Fouché, and T. T. Retief, *Electrochim. Acta, 22,* 391 (1977).
5 O. G. Holmes and D. S. McClure, *J. Chem. Phys., 26,* 1686 (1957).
6 R. F. Fenske, D. S. Martin and K. Ruedenberg, *Inorg. Chem., 1,* 441 (1962).
7 E. T. van der Kouwe and A. von Gruenewaldt, *J. Appl. Electrochem., 7,* 407 (1977).